UNIVERSITY OF CALIFORNIA SAN DIEGO

Decoupled Epineurial and Axonal Deformation in Mouse Median and Ulnar Nerves

A Thesis submitted in partial satisfaction of the requirements for the degree

Master of Science

in

Biology

by

Jaemyoung Sung

Committee in charge:

Sameer Shah, Chair
Brenda Bloodgood, Co-Chair
Ella Tour

2018

The Thesis of Jaemyoung Sung is approved and it is acceptable in quality and form for publication on microfilm and electronically:

_____

_____

Co-Chair

_____

Chair

University of California San Diego

2018

TABLE OF CONTENTS

LIST OF FIGURES

ABSTRACT OF THE THESIS

Decoupled Epineurial and Axonal Deformation in Mouse Median and Ulnar Nerves

by

Jaemyoung Sung

Master of Science in Biology

University of California San Diego, 2018

Dr. Sameer Shah, Chair

Dr. Brenda Bloodgood, Co-Chair

Peripheral nerves span one or more articulating joints, and must accommodate mechanical loads during day-to-day activities. Axons are protected in part by their undulation within the nerve, implied by the Bands of Fontana. In addition, previous studies have identified regions of increased epineurial strain and compliance, particularly near joints. Most of these studies have focused on regional differences in epineurial strain; however, how internal nerve compartments, including the axons, perceive this increased deformation is less understood. Using transgenic mice expressing a fluorescent reporter within their neurons, we tested 1) whether mesoneurial tissue contributes to regional variability in epineurial strain, and 2) whether nerves

increase their local axonal undulation in regions of high epineurial strain, as a strategy to protect nerve fibers from strain-induced damage.

In our results, we observed a decoupling between regions of high epineurial strain and high axonal tortuosity. Consistent with previous studies, decompression resulted in significant differences in regional strain, confirming strong mesoneurial influences on epineurial strain. However, regional differences in axonal tortuosity were largely unchanged by decompression or excision, signaling that epineurial measurements may not fully represent the response of the inner nerve. Based on our findings and previous literatures, we propose a neuromechanical model that permits axons to unravel along their length due to looser coupling between the peri/endoneurium. This capability may result in enhanced axonal protection to injury than suspected. These findings have implications for our understanding of nerve biomechanics as well as the progression of nerve dysfunction due to injury, disease, or surgery.

This abstract is a rephrased version of the material submitted to Muscle and Nerve, titled "Decoupled Epineurial and Axonal Deformation in Mouse Median and Ulnar Nerves" by Sung, Jaemyoung; Sikora-Klak, Jakub; Blevins, Elisabeth; Adachi, Stephanie; Shah, Sameer. The thesis author, Jaemyoung Sung, was the first author of this paper.

ACKNOWLEDGEMENTS

I dedicate this section to express my gratitude towards everyone who has helped me with this project as well as my experience and education in UC San Diego.

This project would not have been possible without my mentor, Dr. Sameer Shah in UCSD, Department of Orthopaedic Surgery. This project being my first major research, I have received invaluable help and advice whenever I ran into trouble in lab. I came into the lab as a novice, and I thank him for helping me throughout the last four years to grow as a scientist.

I would also like to thank all the co-authors who helped push this project forward: Dr. Jakub Sikora-Klak, Ms. Elisabeth Blevins, and Ms. Stephanie Adachi. The troubleshooting, help with animal care, and blind analyses has immensely helped in boosting the quality of this project.

In addition, I want to share my gratefulness for the committee members, Dr. Ella Tour and Dr. Brenda Bloodgood, not only for their critiques and advice on this project, but also for the life-long lessons that I learned from lectures and meetings. It would be an understatement to say that my current interest in biology has been hugely impacted by their passion in science.

This thesis – which includes the abstract, introduction, Chapter 1-5, and figures – is a reprint of the material submitted to Muscle and Nerve, titled. “Decoupled Epineurial and Axonal Deformation in Mouse Median and Ulnar Nerves” by Sung, Jaemyoung; Sikora-Klak, Jakub; Blevins, Elisabeth; Adachi, Stephanie; Shah, Sameer. The thesis author, Jaemyoung Sung, was the first author of this paper.

Thank you.

Author

Jaemyoung Sung

Chapter 1: Introduction

Peripheral nerves experience mechanical loads due to the movement of articulating joints. However, excessive tensile stress on nerves can cause a multitude of neurovascular problems, including structural damage, vascular flow decrease, and conduction deficits (Sunderland 1990, Ogata and Naito 1986, Jou et al. 2000, Clark et al. 1992). Nerve traction has also been implicated in the pathological progression of several entrapment neuropathies, including carpal and cubital tunnel syndromes (Ho and Marmor 1971, Brown, Yates and Ferguson 1980, O'Driscoll et al. 1991, Childress 1956). Therefore, nerves must maintain sufficient compliance to maintain their physiological functions (Sunderland and Bradley 1949). Compounding their biomechanical challenge, nerves experience especially high epineurial strains – and a corresponding increase in compliance – near joints, as reported in a number of animal and human models (Mahan et al. 2015, Phillips et al. 2004, Toby and Hanesworth 1998). In fact, simple tasks such as elbow flexion can introduce ulnar nerve strains of 30% at the elbow (Wright et al. 2001) – a magnitude that far exceeds posited thresholds at which nerves suffer irreversible functional deficits (Clark et al. 1992, Kwan et al. 1992).

These observations raise the important questions of what design features underlie the remarkable ability of nerves to withstand high and variable deformation, and how nerve strain is directed to specific regions along and within the nerve. A number of studies have indicated that axons are at least partially protected by their undulation within the nerve – a pattern that is likely responsible for observed Bands of Fontana (Clarke and Bearn 1972, Rydevik and Nordborg 1980). Though regional differences in such waviness have not been examined in human nerves or typical laboratory animal models, a recent study of nerves in the rorqual whale jaw demonstrated dramatic regional differences in axonal and fascicular undulation depending on

nerve geometry and required elongation (Lillie et al. 2017, Vogl et al. 2015). Connective tissue and fascicular organization have also been implicated in regulating epineurial strain and nerve compliance. In the rat median nerve, thinner and denser collagen fibrils near joint regions were posited to explain increased local compliance, though similar differences were not seen in sciatic nerves (Mason and Phillips 2011). In addition, variability in fascicular number or spacing have also been posited as an explanation for local compliance, though results in support of this hypothesis are conflicting (Phillips et al. 2004, Sunderland and Bradley 1949). More recently, an important role for the mesoneurium (paraneurium) in regulating regional epineurial strains was described in rat sciatic nerves (Foran et al. 2017), suggesting that structures that tether the epineurium to the nerve bed contribute to the response of a nerve to imposed deformation.

Despite this progress, less clear is the degree to which epineurial strain is transmitted to – and thus representative of – strain within internal compartments of the nerve, including the axons. In this study, we used Brainbow mice, which exhibit fluorescence in their neurons (Livet et al. 2007, Weissman et al. 2011a, Weissman et al. 2011b), to investigate the relationship between epineurial and axonal deformation. In particular, we examined the median and ulnar nerves, which have different anatomical trajectories across the elbow, to test the hypothesis that axons increase the frequency of their undulations locally in regions of high epineurial strains. Consistent with previous studies, we observed increased epineurial strain in vicinity of moving joints. However, though axonal waviness varied along the length of the nerve, the pattern of this variability as decoupled from that of the overlying epineurium. These findings have important implications for our understanding of lateral transmission of strain in peripheral nerves, as well as for understanding the progression of nerve dysfunction due to injury, disease, or surgery.

Chapter 1, in full, is a reprint of the material submitted to Muscle and Nerve, titled

“Decoupled Epineurial and Axonal Deformation in Mouse Median and Ulnar Nerves” by Sung, Jaemyoung; Sikora-Klak, Jakub; Blevins, Elisabeth; Adachi, Stephanie; Shah, Sameer. The thesis author, Jaemyoung Sung, was the first author of this paper.

Chapter 2: Methods

2.1 Animals and genotyping

All procedures were approved by the Institutional Animal Care and Use Committee (IACUC) at UCSD. Brainbow (Br; B6.Cg-Tg(Thy1-Brainbow1.0)HLich/J, Jackson Laboratories, Stock# 007901) and Thy-1 Cre (Cre; FVB/N-Tg(Thy1-cre)1Vln/J, Jackson Laboratories, Stock: #006143) mice were acquired commercially, and breeding as well as PCR was performed as recommended by the vendor. Polymerase chain reaction (PCR) on DNA from tail clippings was performed through NaOH-based DNA extraction and per standard methods.

For Cre genotyping, the following vendor-suggested primer sets were used: [oIMR9535] 5'-GCG GTC TGG CAG TAA AAA CTA TC-3' / [oIMR9296] 5'-GTG AAA CAG CAT TGC TGT CAC TT-3' / [oIMR8744] 5'-CTA GGC CAC AGA ATT GAA AGA TCT-3' / [oIMR8745] 5'-GTA GGT GGA AAT TCT AGC ATC ATC C-3' (Cre Forward/ Cre Reverse/Cre-Control Forward/Cre-Control Reverse). For Brainbow genotyping, the following vendor-provided primer set was used: [oIMR1084] 5'-CAA ATG TTG CTT GTC TGG TG-3' / [oIMR1085] 5'-GTC AGT CGA GTG CAC AGT TT-3' / [oIMR7338] 5'-CGC TGA ACT TGT GGC CGT TTA CG-3' / [oIMR7339] 5'-GGG AGG ATT GGG AAG ACA AT-3' (Br Forward/Br Reverse/Br-Control Forward/Br-Control Reverse). All mice positive for Br expressed fluorescence and were used for analysis. Those positive for Br and for Cre expressed red, yellow, and cyan fluorescent protein (RFP, YFP, CFP), while mice positive for Br but negative for Cre expressed RFP alone. 4 to 12-week-old mice were sacrificed by CO2 asphyxiation, and were used for subsequent analysis.

2.2 Exposure and kinematics of ulnar and median nerve

All in situ experiments were completed within 30 minutes of sacrifice. Overlying skin was removed from shoulder to wrist, and clavicular portions of pectoralis major and biceps brachii (short head) were excised. All underlying mesoneurium, which connected ulnar and median nerves to their bed, was left intact. Care was given to minimize the removal of any overlying mesoneurium; however, a portion of overlying soft tissues mid-humerally were removed for clean marking purposes. To expose the ulnar nerve, the flexor carpi ulnaris was fully removed and the flexor digitorium superficialis partially removed for visibility. To expose the median nerve, the pronator teres was excised with flexor carpi radialis partially removed for visibility. Cork pads and pins (Austerlitz Insect Pins, .15mm) were used to keep the arms still during dissection. Isotonic mammalian nerve Ringer's solution (Bober et al. 2015) was used to keep tissues hydrated.

Epineurial strain was measured based on methods previously used in rat sciatic nerves (Foran et al. 2017) and in the human upper extremity (Foran et al. 2016, Mahan et al. 2015). Briefly, a total of five epineurial fiduciary markers were made with 1 mm (ulnar) or 2 mm (median) between each marker to demarcate the region directly overlying the elbow joint, and regions proximal and distal to the joint (Figure 1A- C). For both nerves, markers were centered at the imaginary line connecting the medial and lateral epicondyle, with joints in a configuration placing nerves in a tensioned state. The four regions analyzed were: proximal non-joint (P-NJ), immediately proximal to the center of the joint (P-J), immediately distal to the center of the joint (D-J), and distal non-joint (D-NJ) (Figure 1A). Regional strains were calculated based on marker spacings in a joint configuration that placed the nerves under tension relative to marker spacings for joint configurations in which nerves were untensioned (Figure 1D). Strains were also measured following circumferential decompression of mesoneurial tissue. Only one type of

nerve, either median or ulnar, was used for analysis per mouse to minimize the time per experiment and to ensure consistency in tissue removal. Images of the nerves in two joint configurations were taken using a Leica M60 Microscope, taking care that surface markers were in a single plane to prevent artifacts associated with parallax.

2.3 Ex vivo imaging

The extremity of interest was pinned to tissue culture dishes (Corning, D × H 100 mm × 20 mm) coated with Polydimethylsiloxane (SYLGARD® 184 SILICONE ELASTOMER), fully submerged in Ringer's solution. Nerves were excised proximally and distally to the marked portion in situ, and were either laid a cover slip on top or sutured (Ethilon 8-0 Nylon Sutures) to keep the nerves flat with minimal stretch. Severed nerves were placed within a custom-fabricated tissue-stretching device (Shah and Lieber 2003), which enabled the nerve to be mounted within a Ringer's solution filled chamber and imaged through its clear cover-slipped floor under controlled deformation.

For tortuosity analysis, nerves were held at the minimum tension required to keep the nerves straight without floating. Nerves remained bathed in Ringer's solution throughout the imaging process. All nerves were imaged using a Leica DMI 6000 B confocal microscope with HC PL FLUOTAR 20x/0.5 lens. Fluorescence for RFP, CFP, and YFP was scanned using Z-stacks through the maximum thickness within which fluorescence could be observed. Images reflect 4x line averaging (Figure 2A and B). Each of the four above-designated nerve regions (P-NJ, P-J, D-J, D-NJ) were imaged and Image J (National Institutes of Health) was used to measure up to three different visible axons lengths (L) per nerve with their corresponding nerve lengths (C). We defined tortuosity (τ) as:

$$\tau = \frac{Axon\ Length\ (L)}{Nerve\ Path\ Length\ (C)} \quad (1)$$

A subset of nerves was stretched during imaging, to confirm that axonal undulations disappeared under strain. Within the tissue-stretching chamber, images were captured of nerves before and after 12.5% epineurial strain. In situ nerve images were also compared to ex vivo images on mouse median nerves (N = 4 nerves), to test whether nerve excision affects tortuosity (average of 4 axons per nerve). In situ imaging was performed through an upright widefield fluorescence microscope (Leica DM 6000 B) with HCX PL FLUOTAR 10X/.30 objective. Nerves were imaged both in situ and ex vivo with care given to match surface marker deformation in the relaxed position, as defined in Figure 1D.

2.4 Statistics

Mean regional strains were compared using 2-way unweighted ANOVA (factors: region and decompression), with comparison of individual means post-hoc using Tukey's HSD. Mean tortuosity was compared using 1-way repeated measures ANOVA (factor: region). Significance was indicated for $p<0.05$.

Chapter 2, in full, is a reprint of the material submitted to Muscle and Nerve, titled "Decoupled Epineurial and Axonal Deformation in Mouse Median and Ulnar Nerves" by Sung, Jaemyoung; Sikora-Klak, Jakub; Blevins, Elisabeth; Adachi, Stephanie; Shah, Sameer. The thesis author, Jaemyoung Sung, was the first author of this paper.

Chapter 3: Results

3.1 Effect of decompression on regional epineurial strain

We first examined regional differences in epineurial strain of ulnar and median nerves of Brainbow mice in situ, and the effect of decompression on these strains. ANOVA revealed a significant effect of region on strain in the ulnar nerve ($p<.01$), and a strong trend in the median nerve ($p=0.07$). Prior to decompression, for the median and ulnar nerves, higher strain was observed in joint regions compared to non-joint regions (Figure 1E-F). Post-hoc analysis of ulnar nerve strains revealed significant differences between P-NJ vs. D-J ($p<0.01$) and D-NJ vs. D-J ($p< 0.01$). Strain was particularly high (23.4%) in the D-J region (Figure 1F). Post-hoc analysis of median nerve strains indicated a significant difference between P-NJ and D-J regions ($p<0.05$).

ANOVA also revealed a significant effect of mesoneurial decompression on strain, in both nerves ($p<.05$ for median; $p<.001$ for ulnar), and no interaction effect. Decompression noticeably reduced the strain disparity among regions (Figure 1E-F), with strains in joint regions particularly reduced from their pre-decompression levels (ulnar: $p<0.001$, median: $p<0.01$). Any decreases in strain decrease after decompression may indicate dissipation of strain to proximal or distal regions of the nerve in which we were unable to measure strain.

3.2 Regional differences in axonal tortuosity

We then examined axonal waviness, taking advantage of neuronal fluorescence in Brainbow mice (Figure 2). Axons in both median and ulnar nerves displayed regional variability in tortuosity (ulnar: $p<.01$; median: $p<.001$); However, these regional differences in tortuosity did not match those of epineurial strain. Unlike epineurial strain, axonal tortuosity seemed

independent from proximity to the joint, showing higher tortuosity proximally compared to distally. Post-hoc testing in the median nerve revealed significant differences between P-J and D-J ($p<.01$); P-J and D-NJ ($p<.01$); P-NJ and D-J ($p<.05$). In the ulnar nerve, there was a significant difference in tortuosity between P-NJ and D-J ($p<.05$); P-NJ and D-NJ ($p<.05$). To confirm that the axons indeed unraveled during strain, the axonal undulation of axons in a strained state was compared to that in an unstrained state. For both the median and the ulnar nerve, there was a clear straightening observed in the Brainbow expressing nerves following 12.5% strain (Figure 2E-F). Tortuosity could not be measured in deformed nerves.

Given that nerves in situ may be under slight tension even at apparent slack (Kwan et al. 1992, Walbeehm et al. 2004), we tested the degree to which nerve excision influenced axonal waviness under no tension. Tortuosity of unloaded median nerves ($n = 4$) and multiple axons ($n = 16$) were compared in situ and ex vivo. Minimal differences in tortuosity measurements were observed in situ and ex vivo (Figure 3A), though in situ tortuosity systematically undershot ex vivo tortuosity, excepting the P-J region. Differences were no more than 2.37% in any region (range: 0.77%-2.37%). Importantly, regional gradients in tortuosity were also conserved in situ and ex vivo, suggesting that the mesoneurium (and thus also decompression) does not appreciably influence regional differences in axonal architecture.

A few additional observations are worth noting. First, consistent with previous studies (Clarke and Bearn 1972, Love et al. 2013), axonal waviness was observed to match the Bands of Fontana effect, which emerged in overlaid fluorescence channels (Figure 4A). In addition, a portion of the AIN branch of the median nerve was observed in a subset of excised nerves. In each of these samples, tortuosity was substantially higher than that in the more proximal nerve trunk, suggesting that branch points may experience a unique loading environment (Figure 4B).

Finally, though there was no systematic pattern, we frequently observed axons crossing over each other in the same confocal plane (Figure 2A), suggesting that axons do not necessarily travel in the same fascicles or sub-fascicles within a given region.

Chapter 3, in full, is a reprint of the material submitted to Muscle and Nerve, titled "Decoupled Epineurial and Axonal Deformation in Mouse Median and Ulnar Nerves" by Sung, Jaemyoung; Sikora-Klak, Jakub; Blevins, Elisabeth; Adachi, Stephanie; Shah, Sameer. The thesis author, Jaemyoung Sung, was the first author of this paper.

Figure 1. Tensile Strain Testing Schematics and Results

(A) Demarcation schematic for both ulnar and median nerves. Confocal images of axonal fluorescence in Brainbow mice were taken individually in every region as represented in green "Image Area."

(B-C) Median nerve images in the stretched state (B) and relaxed state (C).

(D) Limb positions used for stretched and relaxed state in each nerve. Shoulder adduction angle was set to 0° for all strain measurements using appropriate cork pads under the limbs.

(E-F) Strain measurement results. Error bars indicate standard error. **: $p<.01$, *: $p<.05$. Black lines above the bar graph show post-hoc sigficance in regional difference. Asterisks above the gray bars show post-hoc significance between decompressed and non-decompressed strain.

(E) Sample size for median nerve groups: n(Non-Decompressed) = 10, n(Decompressed) = 6.

(F) Sample size for ulnar nerve groups: n(Non-Decompressed) = 7, n(Decompressed) = 7.

A.

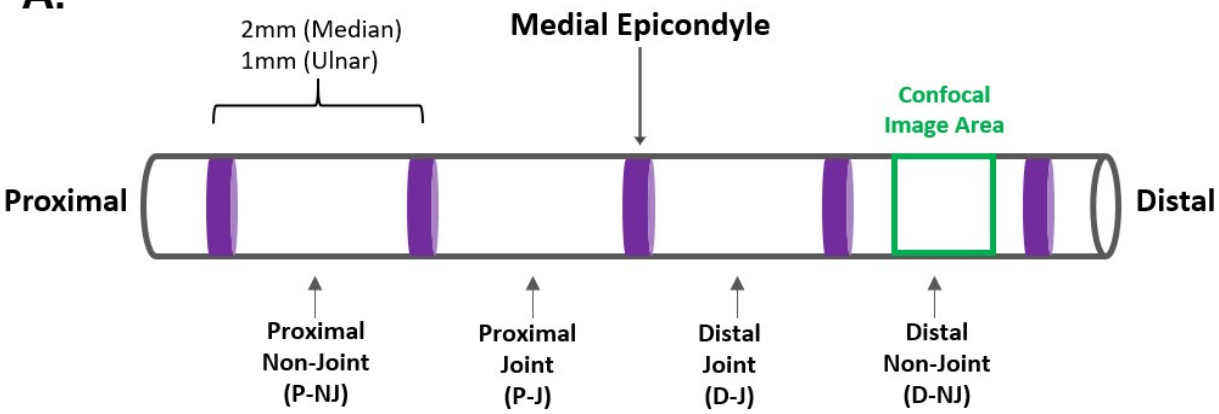

B.

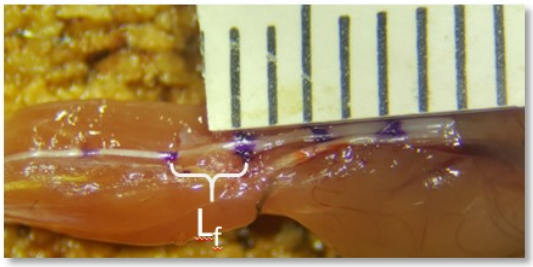

C.

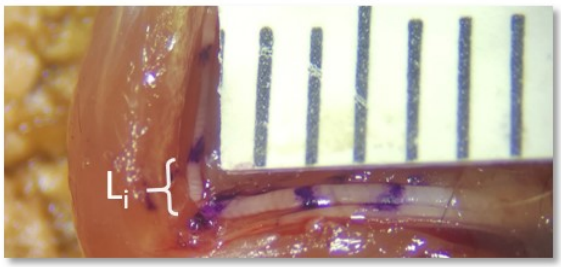

D.

Nerve	State	Elbow	Wrist/Palm
Median	Stretched	0°	Ventral
	Relaxed	90°	Ventral
Ulnar	Stretched	90°	Medial
	Relaxed	0°	Medial

E.

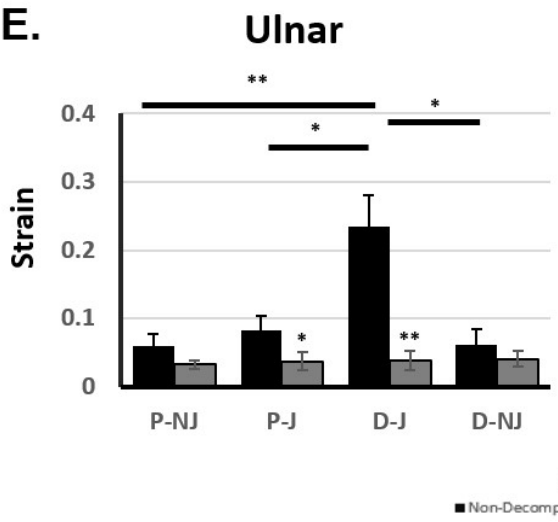

F.

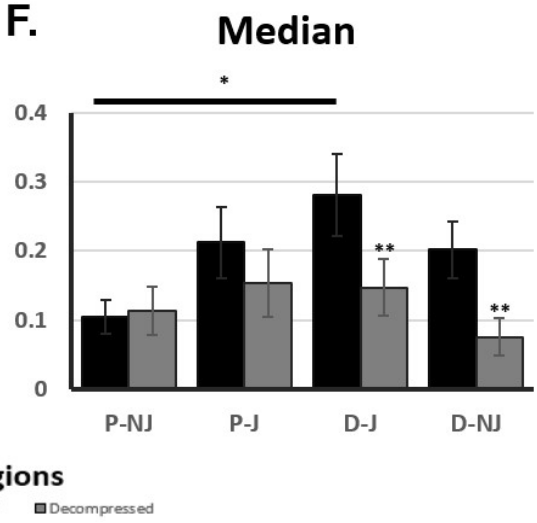

Figure 2. Axonal Tortuosity Measurements and its Response to Strain

(A) A Br+/Cre- ulnar nerve expressing RFP. Visible axons were used to measure tortuosity. Scale bars = 200um.

(B) An overlay-image of an Br+/Cre+ median nerve expressing both CFP (green) and RFP (red). Green arrow marks axons expressing YFP and red arrow marks axons expressing RFP. Unknown artifact shown in white arrow. Scale bars = 200um.

(C-D) Tortuosity measurement results. Error bars indicate standard error. Sample size (axons) is indicated in the parentheses next to the regions. **: $p<.01$, *: $p<.05$. Black lines above the bar graph indicates post-hoc significance between the regions.

(C) Mean axonal tortuosity observed in median nerves. P-NJ: 1.028; P-J: 1.036; D-J: 1.018; D-NJ: 1.022

(D) Mean axonal tortuosity observed in ulnar nerves. P-NJ: 1.034 / P-J: 1.024 / D-J: 1.016 / D-NJ: 1.016

(E-F) Axon tortuosity pattern changes under no strain (E) and 12.5% strain (F). Images shown are examples of the P-NJ region of a median nerve. Scale bars = 200um.

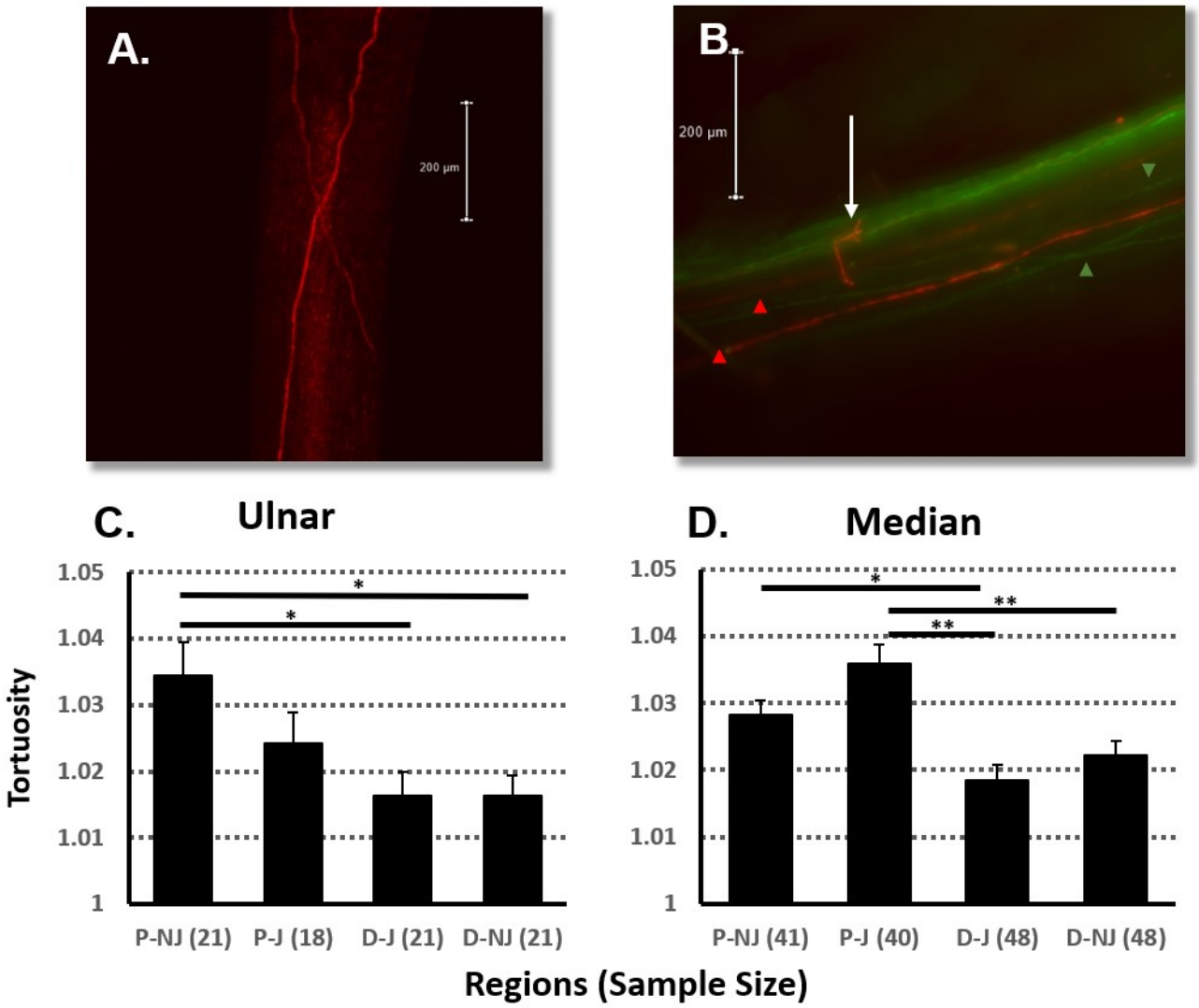
A.
200 µm
B.
200 µm
C.
Ulnar
D.
Median
Tortuosity
1.05
1.04
1.03
1.02
1.01
1
*
*
**
**
P-NJ (21)
P-J (18)
D-J (21)
D-NJ (21)
P-NJ (41)
P-J (40)
D-J (48)
D-NJ (48)
Regions (Sample Size)

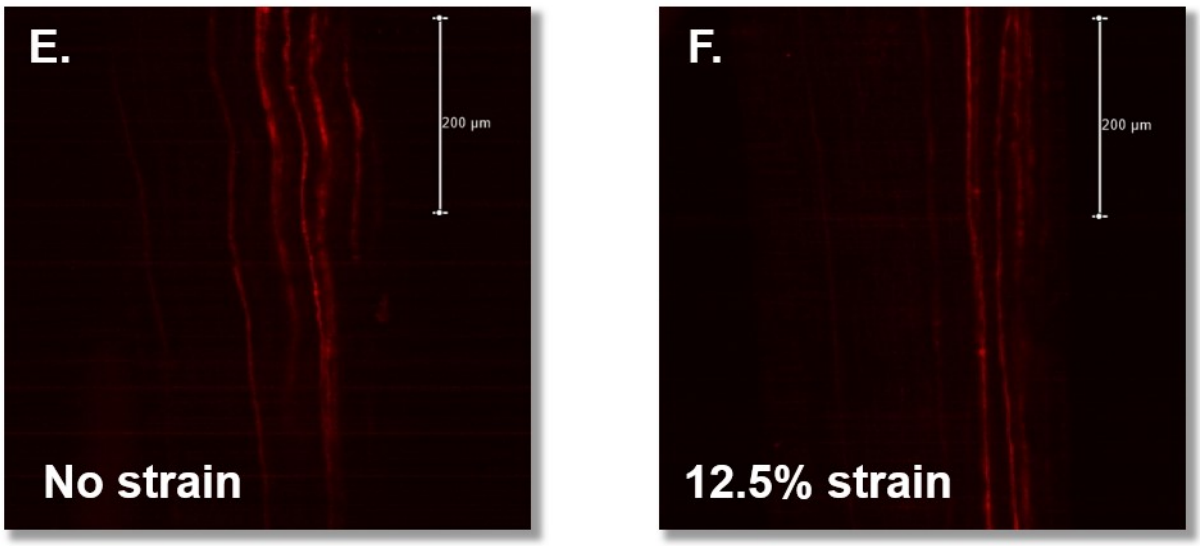
E.
200 µm
No strain
F.
200 µm
12.5% strain

Chapter 4: Discussion

In this study, we examined regional differences in epineurial strain and axonal architecture in mouse median and ulnar nerves at the elbow, using a Brainbow transgenic mouse model. Nerve lengthening in situ and ex vivo induced epineurial strain and unraveling of axonal undulations. However, surprisingly and contrary to our original hypothesis, which posited increased axonal undulation in regions of high epineurial strain, we observed that regions of high axonal tortuosity did not correspond to regions of high epineurial strain. In addition, mesoneurial decompression markedly reduced regional heterogeneity in epineurial strain, but did not affect axonal tortuosity. This apparent decoupling between the mechanical response of the epineurium and internal compartments of the nerve has important implications for understanding lateral force-transmission in nerves as well as understanding biomechanical and structural impacts of peripheral nerve surgery.

4.1 Mesoneurial effects on epineurial strain distribution

Previous studies in median and ulnar nerves in rat models and humans revealed higher strains in the joint regions of the nerve (Mahan et al. 2015, Phillips, Hill and Atherton 2012, Toby and Hanesworth 1998), with maximum strains ranging from 20-30%. We observed similar distributions and magnitudes of strain in both median and ulnar nerves at the elbow, most prominently in the distal joint (D-J) region (Figure 1E and F). These data are the first such reported in mice, which may ultimately prove to be a valuable surgical model due to the potential for their genetic manipulation.

The observed homogenization of strain distributions after decompressing the mesoneurium (Figure 1E and F) is consistent with a similar redistribution observed in rat sciatic

nerves and in patients with cubital tunnel syndrome following circumferential decompression (Foran et al. 2017, Foran et al. 2016). The concurrent reduction in strain, also noted in (Foran et al. 2017) albeit to a lesser extent, is likely due to the longitudinal relocation of the strain to proximal or distal regions that could not be visualized. Alternatively, though we did not observe obvious subluxation of the nerve during joint manipulation, reduced strain may also reflect subtle alterations to the nerve course through its bed.

4.2 Decoupled regional variability in axonal tortuosity and epineurial strain

Axons have been described in many models to follow a wavy trajectory. For example, rat sciatic nerves and rabbit brachial plexi revealed wavy nerve fibers under high magnification, and the disappearance of the Bands of Fontana phenomenon during deformation hints to an unraveling of nerve fibers (Clarke and Bearn 1972, Merolli, Mingarelli and Rocchi 2012). More dramatically, a highly wavy architecture was observed to underlie nerve compliance in Rorqual whales (Lillie et al. 2017, Vogl et al. 2015). Based on these and related findings, there is ample evidence that axons utilize their waviness to withstand nerve deformation. Using Brainbow transgenic mice, we were able to image and more reliably examine three-dimensional trajectories of axons, including the assessment of tortuosity, free of any confounding factors resulting from sectioning tissue. We also observed consistent alignment of spiral Band of Fontana (BoF) with axonal undulations (Figure 4A), in support of previous literature (Clarke and Bearn 1972, Love et al. 2013, Merolli et al. 2012). Further, within feasible imaging depths, these undulations appeared to be planar, even when reconstructed confocally. Such alignment of planar waves was similar to that observed by Clarke and Bearn in the rat brachial plexus (Clarke and Bearn 1972),

and suggests that any posited helical coiling of nerve fibers (Merolli et al. 2012), is likely to be relatively gentle, if at all.

We initially hypothesized that such axonal waviness would vary regionally, to match higher epineurial strains and increased compliance near articulating joints. As we posited, axons in both median and ulnar nerves exhibited a wavy phenotype, and their tortuosity varied regionally. Consistent with a role in providing strain relief, axonal waviness disappeared with nerve deformation. Contrary to our initial hypothesis, though, we did not observe higher tortuosity in regions of high epineurial strain. Instead, while epineurial strain was highest near joints, tortuosity generally increased proximally (Figure 2C-D). Thus, though both the epineurium and axons are mechanically loaded during nerve stretch or joint movement, the interior of the nerve does not appear to sense strain in the same manner as the epineurium. In fact, high epineurial strain regions such as the distal joint (D-J) region display a low level of axonal tortuosity (Figures 1E-F, 2C-D).

These findings suggest different mechanisms of coping with deformation in different regions of the nerve, as well as a level of decoupling between the epineurium and axons. Several findings in the literature have hinted at such decoupling. First, a severed nerve displays a mushrooming effect, suggestive of some slippage between layers of the nerve (Georgeu et al. 2005, Walbeehm et al. 2004). Also, typical of composite biological tissues in general, a toe-region also exists in the stress-strain curves of nerves, within which strain can be applied to the nerves with negligible stress borne by the nerve, suggesting compliance in load-bearing elements of the nerve (Kwan et al. 1992, Sunderland and Bradley 1949). The epineurium and perineurium are the most likely candidates for load-bearing. In one study, peeling of the epineurium of rat sural nerves decreased nerve modulus by up to 5x, with the perineurium intact (Bober and Shah

2015). On the other hand, the perineurium -- which consists of collagen, elastic fibers, and the basal lamina (Georgeu et al. 2005, Sunderland 1990) – has also been posited as the major load bearing layer of the nerve; indeed, rabbit tibial nerves lost most of their load bearing capabilities with perineurial breakage at strains of 27% beyond in situ strain (Rydevik et al. 1990). In both of these studies, as well as others (Jou et al. 2000, Wall et al. 1992), the endoneurium and axons were spared under nerve tension, suggesting that axons did not sense or bear the same loads as surrounding connective tissue (Rydevik et al. 1990, Sunderland 1990). The finding that nerves maintain similar mechanical properties after Wallerian degeneration further supports the idea that the axonal compartment minimally contributes to nerve biomechanical properties (Sunderland and Bradley 1961).

This decoupling may offer some protection to axons, which are structurally continuous along their entire length, from their cell body to their termini. Thus, while loads transmitted laterally via connective tissue and/or myelin may subtly influence axonal deformation locally, the entire length of the axon may be used to dissipate strain. The rationale for increased axonal tortuosity proximally is not clear. It is possible that there is more inherent capacity for undulation in monofascicular regions of nerves; however, the observation of increased tortuosity in the branch points (e.g., AIN branch, Figure 4B) suggests that the design constraints on axonal tortuosity are more complex.

4.3 A model for connectivity between layers of the nerve

On one hand, there must be connectivity between each layer of the nerve. Our observations that mesoneurial decompression affects epineurial strain imply a coupled meso-epineurium (Figure 5A, (Foran et al. 2017)). Additionally, previous literature dictates that

physical viscoelastic connections at the core-sheath interface (Georgeu et al. 2005, Tillett et al. 2004), which disallow excessive epi-perineurial gliding. Finally, the endoneurium and nerve fiber must be coupled to the perineurium. This possibility is supported by our observations that joint manipulation and ex vivo loading indeed result in the unraveling of axonal undulations, by previous observations of connections between myelin and endoneurial collagen, and endoneurial fibers and the perineurium (Gamble 1964, Gamble and Eames 1964, Thomas 1963), and by the fact that individual nerve fibers are not readily peeled from their fascicles during fine dissection. However, for internal gliding of nerve fibers to occur, any connections between endoneurial connective tissue to the perineurium must be highly compliant. As axonal undulations are restored after cyclic loading, these connections must also be highly elastic. Based on our observations and previous literature on nerve architecture, we propose a nerve model with a tightly coupled meso-epi-perineurium, but a loosely coupled peri-endoneurium that allows axons to glide and unravel throughout the length of the nerve (Figure 5B). While our data do not speak to such a possibility, we also propose connectivity between successive undulations, to enable the consistent recoil of axons into their original wavy configuration.

Chapter 4, in full, is a reprint of the material submitted to Muscle and Nerve, titled "Decoupled Epineurial and Axonal Deformation in Mouse Median and Ulnar Nerves" by Sung, Jaemyoung; Sikora-Klak, Jakub; Blevins, Elisabeth; Adachi, Stephanie; Shah, Sameer. The thesis author, Jaemyoung Sung, was the first author of this paper.

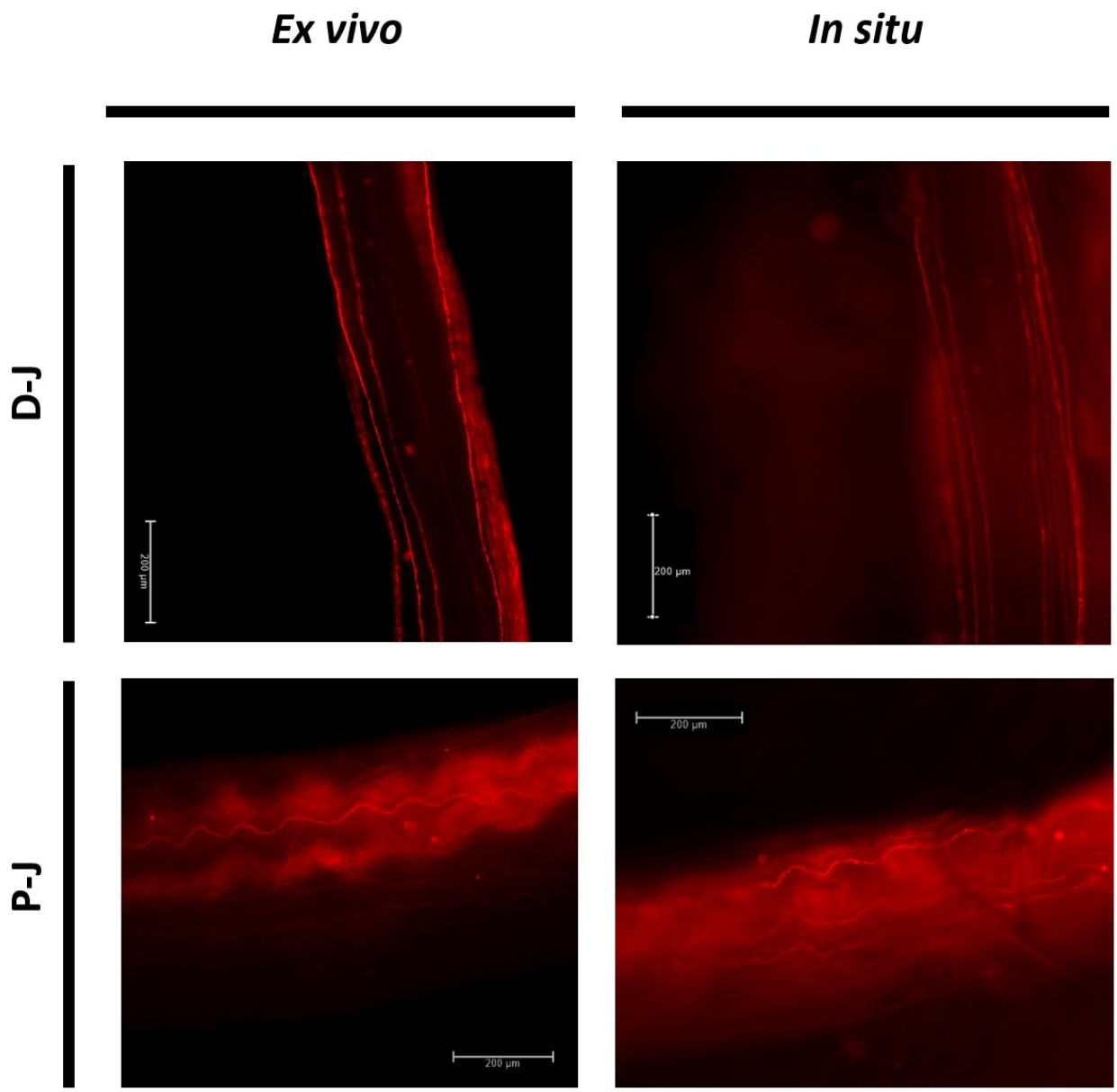

Figure 3. Mesoneurial Effects on Axonal Tortuosity
Representative RFP images of a median nerve under mesoneurial influences (in situ) and without (ex vivo). In situ measurements were done in the relaxed configuration as defined in Figure 1D. Scale bars = 200um.

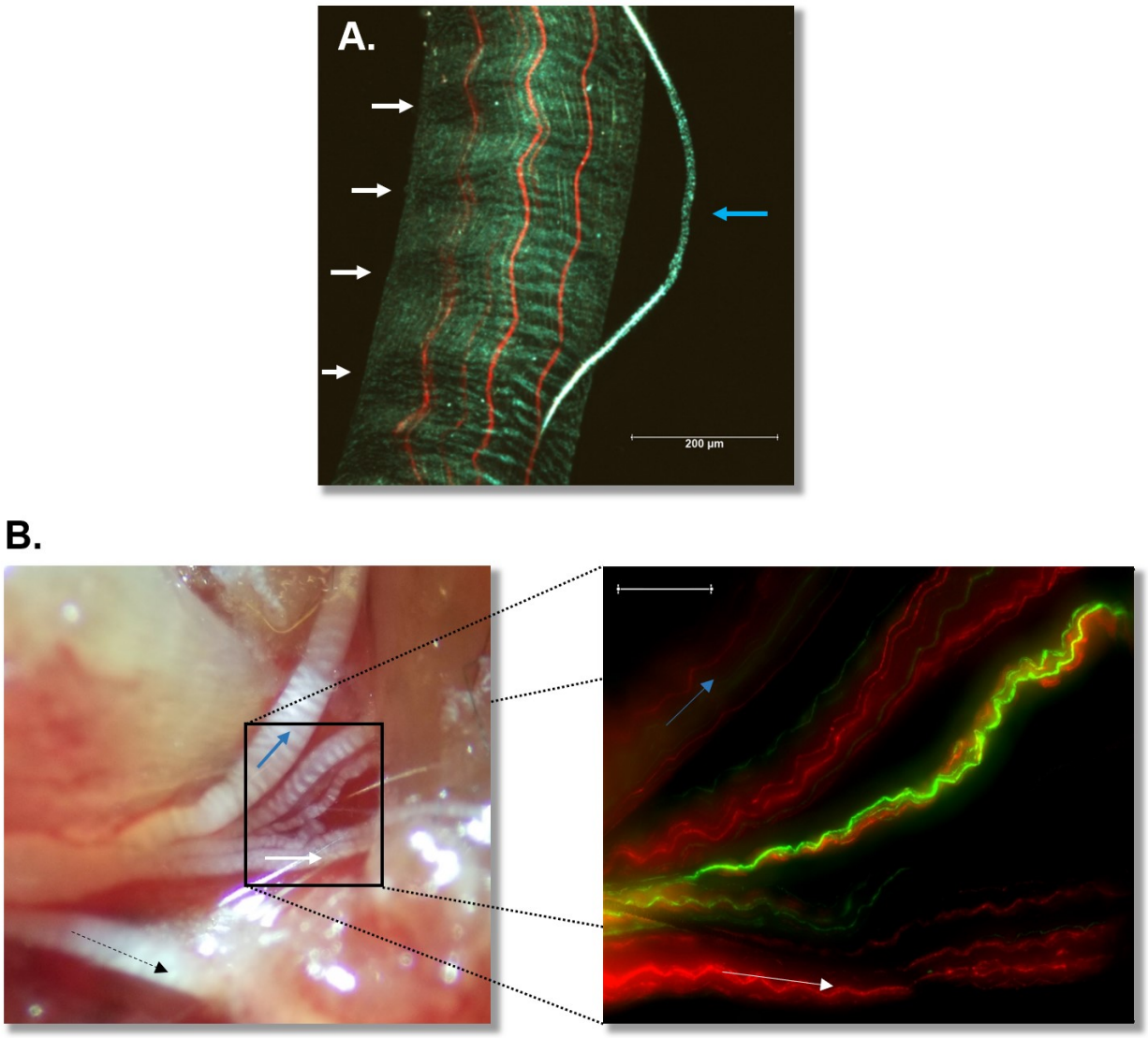

Figure 4. Band of Fontana and Nerve Branching
(A) RFP and CFP overlaid image of Br+/Cre- ulnar nerve. White arrows mark the periodicity of Band of Fontana. Blue arrow marks a hair follicle captured in the image. Scale bar = 200um
(B) Representation of median nerve branches as well as their axon trajectories. Blue arrow indicates the median nerve and the white arrow indicates the main trunk of the AIN. Smaller branches of the AIN were also observed. Compared to the median nerve, the branches show higher tortuosity. Scale bar = 200um

Figure 5 Decoupled Endo-Perineurium Nerve Model and its Response to Stretch

(A) A proposed model of nerve layer connections. Between the nerve bed, epineurium, and perineurium, there are physical connections (mesoneurium and core-sheath interface) that disallow excessive gliding of the nerve. The lack of tight physical connection is represented by the shaded area in the endoneurium.

(B) Response to stretch will differ due to the lack of connection between the nerve fibers and the perineurium. Purple spots represent epineurial markers and red spots represent a hypothetical marker on axons. While the epineurium is limited in movement by the mesoneurium, the axons are relatively free to glide, and the axons on the stretched nerves expand beyond the illustration. In addition, outer layers, such as the epineurium and perineurium, resist breakage through mechanical compliance (represented by the thickness of the outlines), but axons counteract stretch via unraveling.

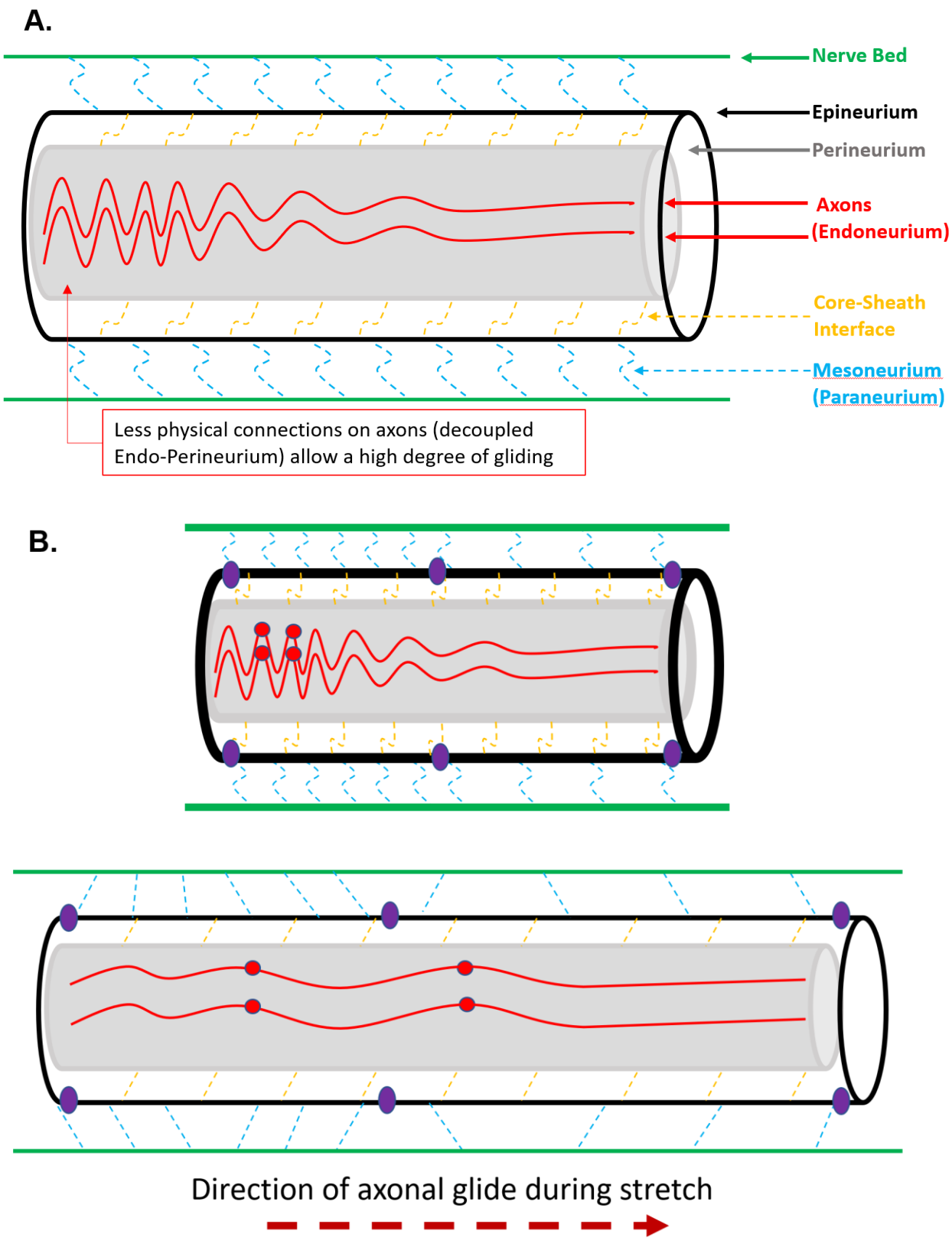
A.
Nerve Bed
Epineurium
Perineurium
Axons
(Endoneurium)
Core-Sheath
Interface
Mesoneurium
(Paraneurium)
Less physical connections on axons (decoupled Endo-Perineurium) allow a high degree of gliding
B.
Direction of axonal glide during stretch

Chapter 5: Conclusion

We observed deformation of both the epineurium and axons at physiological levels of nerve strain. However, differences in the regional patterns of high epineurial strain and increased axonal tortuosity suggest that axons are not fully coupled to outer connective tissue layers of nerves. Thus, while consideration of nerve strain should remain an important factor in treating nerve injuries (Bushnell et al. 2008, Rinker and Liau 2011, Siemionow and Brzezicki 2009), axons may be better protected and less susceptible to traction-induced than suspected. In addition, epineurial strain is likely to be a poor approximation of strains felt by internal compartments of the nerve, including axons; thus, methods to quantify intra-nerve strain are thus of high importance. Looking forward, concepts within this study warrant additional consideration in the context of injured or diseased nerve, where coupling between the inside and outside of a nerve may change, as well as repaired or stretched nerves (Hentz et al. 1993, McDonald and Bell 2010, Vaz, Brown and Shah 2014, Abe et al. 2004, Yokota et al. 2003), where axonal undulations may be altered or eliminated. Such studies have important implications for nerve injury, disease, and repair.

Chapter 5, in full, is a reprint of the material submitted to Muscle and Nerve, titled "Decoupled Epineurial and Axonal Deformation in Mouse Median and Ulnar Nerves" by Sung, Jaemyoung; Sikora-Klak, Jakub; Blevins, Elisabeth; Adachi, Stephanie; Shah, Sameer. The thesis author, Jaemyoung Sung, was the author of this paper.

References

Abe, I., N. Ochiai, H. Ichimura, A. Tsujino, J. Sun & Y. Hara (2004) Internodes can nearly double in length with gradual elongation of the adult rat sciatic nerve. *J Orthop Res,* 22**,** 571-7.

Bober, B. G., E. Gutierrez, S. Plaxe, A. Groisman & S. B. Shah (2015) Combinatorial influences of paclitaxel and strain on axonal transport. *Exp Neurol,* 271**,** 358-67.

Bober, B. G. & S. B. Shah (2015) Paclitaxel alters sensory nerve biomechanical properties. *J Biomech,* 48**,** 3568-76.

Brown, W. F., S. K. Yates & G. G. Ferguson (1980) Cubital tunnel syndrome and ulnar neuropathy. *Ann Neurol,* 7**,** 289-90.

Bushnell, B. D., A. D. McWilliams, G. B. Whitener & T. M. Messer (2008) Early clinical experience with collagen nerve tubes in digital nerve repair. *J Hand Surg Am,* 33**,** 1081-7.

Childress, H. M. (1956) Recurrent ulnar-nerve dislocation at the elbow. *J Bone Joint Surg Am,* 38-A**,** 978-84.

Clark, W. L., T. E. Trumble, M. F. Swiontkowski & A. F. Tencer (1992) Nerve tension and blood flow in a rat model of immediate and delayed repairs. *J Hand Surg Am,* 17**,** 677-87.

Clarke, E. & J. G. Bearn (1972) The spiral nerve bands of Fontana. *Brain,* 95**,** 1-20.

Foran, I., V. Hussey, R. A. Patel, J. Sung & S. B. Shah (2017) Native paraneurial tissue and paraneurial adhesions alter nerve strain distribution in rat sciatic nerves. *Journal of Hand Surgery (European Volume),* in press.

Foran, I., K. Vaz, J. Sikora-Klak, S. R. Ward, E. R. Hentzen & S. B. Shah (2016) Regional Ulnar Nerve Strain Following Decompression and Anterior Subcutaneous Transposition in Patients With Cubital Tunnel Syndrome. *J Hand Surg Am,* 41**,** e343-e350.

Gamble, H. J. (1964) Comparative Electron-Microscopic Observations on the Connective Tissues of a Peripheral Nerve and a Spinal Nerve Root in the Rat. *J Anat,* 98**,** 17-26.

Gamble, H. J. & R. A. Eames (1964) An Electron Microscope Study of the Connective Tissues of Human Peripheral Nerve. *J Anat,* 98**,** 655-63.

Georgeu, G. A., E. T. Walbeehm, R. Tillett, A. Afoke, R. A. Brown & J. B. Phillips (2005) Investigating the mechanical shear-plane between core and sheath elements of peripheral nerves. *Cell Tissue Res,* 320**,** 229-34.

Hentz, V. R., J. M. Rosen, S. J. Xiao, K. C. McGill & G. Abraham (1993) The nerve gap dilemma: a comparison of nerves repaired end to end under tension with nerve grafts in a primate model. *J Hand Surg Am,* 18**,** 417-25.

Ho, K. C. & L. Marmor (1971) Entrapment of the ulnar nerve at the elbow. *Am J Surg,* 121**,** 355-6.

Jou, I. M., K. A. Lai, C. L. Shen & Y. Yamano (2000) Changes in conduction, blood flow, histology, and neurological status following acute nerve-stretch injury induced by femoral lengthening. *J Orthop Res,* 18**,** 149-55.

Kwan, M. K., E. J. Wall, J. Massie & S. R. Garfin (1992) Strain, stress and stretch of peripheral nerve. Rabbit experiments in vitro and in vivo. *Acta Orthop Scand,* 63**,** 267-72.

Lillie, M. A., A. W. Vogl, K. N. Gil, J. M. Gosline & R. E. Shadwick (2017) Two levels of waviness are necessary to package the highly extensible nerves in rorqual whales. *Current Biology*.

Livet, J., T. A. Weissman, H. Kang, R. W. Draft, J. Lu, R. A. Bennis, J. R. Sanes & J. W. Lichtman (2007) Transgenic strategies for combinatorial expression of fluorescent proteins in the nervous system. *Nature,* 450**,** 56-62.

Love, J. M., T.-H. Chuang, R. L. Lieber & S. B. Shah (2013) Nerve strain correlates with structural changes quantified by Fourier analysis. *Muscle Nerve, 48***,** 433-5.

Mahan, M. A., K. M. Vaz, D. Weingarten, J. M. Brown & S. B. Shah (2015) Altered Ulnar Nerve Kinematic Behavior in a Cadaver Model of Entrapment. *Neurosurgery,* 76**,** 747-755.

Mason, S. & J. B. Phillips (2011) An ultrastructural and biochemical analysis of collagen in rat peripheral nerves: the relationship between fibril diameter and mechanical properties. *J Peripher Nerv Syst,* 16**,** 261-9.

McDonald, D. S. & M. S. Bell (2010) Peripheral nerve gap repair facilitated by a dynamic tension device. *Can J Plast Surg,* 18**,** e17-9.

Merolli, A., L. Mingarelli & L. Rocchi (2012) A more detailed mechanism to explain the "bands of Fontana" in peripheral nerves. *Muscle Nerve,* 46**,** 540-7.

O'Driscoll, S. W., E. Horii, S. W. Carmichael & B. F. Morrey (1991) The cubital tunnel and ulnar neuropathy. *J Bone Joint Surg Br,* 73**,** 613-7.

Ogata, K. & M. Naito (1986) Blood flow of peripheral nerve effects of dissection, stretching and compression. *J Hand Surg Br,* 11**,** 10-4.

Phillips, B. E., D. S. Hill & P. J. Atherton (2012) Regulation of muscle protein synthesis in humans. *Curr Opin Clin Nutr Metab Care,* 15**,** 58-63.

Phillips, J. B., X. Smit, N. De Zoysa, A. Afoke & R. A. Brown (2004) Peripheral nerves in the rat exhibit localized heterogeneity of tensile properties during limb movement. *J Physiol,* 557**,** 879-87.

Rinker, B. & J. Y. Liau (2011) A prospective randomized study comparing woven polyglycolic acid and autogenous vein conduits for reconstruction of digital nerve gaps. *J Hand Surg Am,* 36**,** 775-81.

Rydevik, B. & C. Nordborg (1980) Changes in nerve function and nerve fibre structure induced by acute, graded compression. *J Neurol Neurosurg Psychiatry,* 43**,** 1070-82.

Rydevik, B. L., M. K. Kwan, R. R. Myers, R. A. Brown, K. J. Triggs, S. L. Woo & S. R. Garfin (1990) An in vitro mechanical and histological study of acute stretching on rabbit tibial nerve. *J Orthop Res,* 8**,** 694-701.

Shah, S. B. & R. L. Lieber (2003) Simultaneous imaging and functional assessment of cytoskeletal protein connections in passively loaded single muscle cells. *J Histochem Cytochem,* 51**,** 19-29.

Siemionow, M. & G. Brzezicki (2009) Chapter 8: Current techniques and concepts in peripheral nerve repair. *Int Rev Neurobiol,* 87**,** 141-72.

Sunderland, S. (1990) The anatomy and physiology of nerve injury. *Muscle Nerve,* 13**,** 771-84.

Sunderland, S. & K. C. Bradley (1949) The cross-sectional area of peripheral nerve trunks devoted to nerve fibers. *Brain,* 72**,** 428-49.

--- (1961) Stress-strain phenomena in denervated peripheral nerve trunks. *Brain,* 84**,** 125–127.

Thomas, P. K. (1963) The connective tissue of peripheral nerve: an electron microscope study. *J Anat,* 97**,** 35-44.

Tillett, R. L., A. Afoke, S. M. Hall, R. A. Brown & J. B. Phillips (2004) Investigating mechanical behaviour at a core-sheath interface in peripheral nerve. *J Peripher Nerv Syst,* 9**,** 255-62.

Toby, E. B. & D. Hanesworth (1998) Ulnar nerve strains at the elbow. *J Hand Surg Am,* 23**,** 992-7.

Vaz, K. M., J. M. Brown & S. B. Shah (2014) Peripheral nerve lengthening as a regenerative strategy. *Neural Regen Res,* 9**,** 1498-501.

Vogl, A. W., M. A. Lillie, M. A. Piscitelli, J. A. Goldbogen, N. D. Pyenson & R. E. Shadwick (2015) Stretchy nerves are an essential component of the extreme feeding mechanism of rorqual whales. *Curr Biol,* 25**,** R360-1.

Walbeehm, E. T., A. Afoke, T. de Wit, F. Holman, S. E. Hovius & R. A. Brown (2004) Mechanical functioning of peripheral nerves: linkage with the "mushrooming" effect. *Cell Tissue Res,* 316**,** 115-21.

Wall, E. J., J. B. Massie, M. K. Kwan, B. L. Rydevik, R. R. Myers & S. R. Garfin (1992) Experimental stretch neuropathy. Changes in nerve conduction under tension. *J Bone Joint Surg Br,* 74**,** 126-9.

Weissman, T. A., J. R. Sanes, J. W. Lichtman & J. Livet (2011a) Generating and imaging multicolor Brainbow mice. *Cold Spring Harb Protoc,* 2011**,** 763-9.

--- (2011b) Generation and imaging of Brainbow mice. *Cold Spring Harb Protoc,* 2011**,** 851-6.

Wright, T. W., F. Glowczewskie, Jr., D. Cowin & D. L. Wheeler (2001) Ulnar nerve excursion and strain at the elbow and wrist associated with upper extremity motion. *J Hand Surg Am,* 26**,** 655-62.

Yokota, A., M. Doi, H. Ohtsuka & M. Abe (2003) Nerve conduction and microanatomy in the rabbit sciatic nerve after gradual limb lengthening-distraction neurogenesis. *J Orthop Res,* 21**,** 36-43.